Appl. Phys. B 48, 67–72 (1989)

Applied Physics B Photophysics and Laser Chemistry

Relativistic Doppler Effect in $^{199}Hg^+$ Stored Ions Atomic Frequency Standard

C. Meis, M. Jardino, B. Gely, and M. Desaintfuscien

Laboratoire de l'Horloge Atomique, Equipe de Recherche du CNRS associée à l'Université Paris Sud, Bâtiment 221, F-91405 Orsay, France

Received 16 May 1988/Accepted 4 July 1988

Abstract. RF traps are widely used nowadays in high resolution hyperfine spectroscopy. The spectrum of the microwave hyperfine transition at 40.5 GHz of the fundamental level $^2S_{1/2}$ of $^{199}Hg^+$ is phase modulated at the secular frequency of the stored ions and it consists of a narrow central line and lateral bands broadened by the ion trajectory and velocity distribution. The central line itself is shifted by the second-order Doppler effect which is the most important systematic error of stored ions frequency standards. In this paper the relativistic Doppler effect in the case of $^{199}Hg^+$ stored ions is deduced applying a mathematical formalism and using physical parameters that we have measured experimentally.

PACS: 32, 35

In the case of an RF trap [1, 2] the ions are confined by an inhomogeneous electric field created inside the trap by a voltage $V = V_{DC} + V_{AC}\cos\Omega t$ applied on the trap electrodes. For a cylindrical trap, which is the case in our experiments, the instantaneous electric potential can be written in cylindrical coordinates [3, 4]:

$$\psi(\varrho, z, t) = (V_{DC} + V_{AC}\cos\Omega t)\frac{2r_0}{z_0}\sum_{p=0}^{\infty}\frac{(-1)^p}{m_p} \times \cos\left(m_p\frac{z}{r_0}\right)\frac{I_0\left(m_p\dfrac{\varrho}{r_0}\right)}{I_0(m_p)}, \quad (1)$$

where r_0 and z_0 are the radius and the half height of the trap, $m_p = \pi\dfrac{r_0}{z_0}\left(p+\dfrac{1}{2}\right)$, and I_0 is the modified Bessel function of first kind of zero order:

$$I_0(\alpha) = \sum_{k=0}^{\infty}(-1)^k(i\alpha)^{2k}/2^{2k}k!\,\Gamma(k+1). \quad (2)$$

The confining properties of (1) have been studied numerically by solving the Mathieu equations of motion of a single ion in the trap [5, 6]. The ion undergoes a small amplitude oscillation (micromotion) at the frequency $\Omega/2\pi$, superimposed on large thermally excited periodic orbits (secular motion) at frequency $\omega_s/2\pi$, governed by an effective potential. In the adiabatic case ($\omega_s \ll \Omega$) the effective potential is given by [7]:

$$V_{eff}(\varrho, z) = V_{DC}\frac{\psi(\varrho, z, t)}{V} + \frac{qV_{AC}^2}{4m\Omega^2}\left[-\nabla\frac{\psi(\varrho, z, t)}{V}\right]^2, \quad (3)$$

where m and q are the ion mass and charge.

The harmonicity and sphericity of (3) have been studied numerically [3]. It has been argued that this effective potential cannot be perfectly spherically symmetrical and the condition of an approximate sphericity in the central space of the trap can be expressed in terms of the components of the trapping voltage:

$$V_{DC} = 0.74\sqrt{2}qV_{AC}^2/m\Omega^2(r_0^2 + 2z_0^2). \quad (4)$$

Under these conditions, the macromotion secular frequency is

$$\omega_S = 2.22qV_{AC}/m\Omega(r_0^2 + 2z_0^2). \quad (5)$$

Assuming a Maxwellian distribution of charge density of a thermalized spherical ion cloud it has been shown

[8] that the total effective potential including space charge is:

$$V_{\text{eff}}(r)=\frac{1}{2}m\omega_s^2 r^2+\frac{Nq^2}{4\pi\varepsilon_0}\frac{1}{r}\operatorname{erf}\left(\frac{r}{R}\right) \tag{6}$$

where ω_s is given by (5), N the total number of stored ions in thermal equilibrium, ε_0 the vacuum permittivity and R a parameter such that $\ln\left[\frac{n(0)}{n(R)}\right]=1$ with $n(0)$ the ion cloud central density.

The mean amplitude of the secular motion is comparable to R and depends directly on the ion temperature. The frequency of the hyperfine splitting of the fundamental level $^2S_{1/2}$ of $^{199}Hg^+$ is 40.5 GHz which corresponds to a wavelength of $\lambda=7.4$ mm of the same order of magnitude as R. Thus the microwave excitation seen by an ion oscillating at $\omega_m/2\pi$, which is the secular frequency reduced by space charge effects [9], is phase modulated at this frequency. The microwave spectrum consists then of well separated lateral bands spaced at $\omega_m/2\pi$ [10]. The central carrier is unshifted and unbroadened by first-order Doppler effect. In this way extremely high precision hyperfine spectroscopy has been carried out [11–13] that led to high performance stored ions atomic frequency standards and especially that of $^{199}Hg^+$ ions [14, 15].

In order to improve the precision of this type of standard an analytic formalism has been developed [8] which accounts for the second-order Doppler shift. When $\omega_m \geqq \omega_s/2$ the macromotion temperature is given as a function of the total number of ions N and of the measured secular frequency $\omega_m/2\pi$:

$$T=N^{2/3}\left(\frac{m\omega_m^2}{2\pi K_B}\right)\left(\frac{q^2|\mu|}{m\varepsilon_0(\omega_s^2-\omega_m^2)}\right)^{2/3} \tag{7}$$

where $\mu=-0.23$ and K_B is the Boltzmann's constant. The contribution of both micromotion and macromotion to the second-order Doppler shift can be written

$$\frac{\Delta f}{f}=-\frac{K_B T}{mc^2}\left(\frac{3}{2}+\frac{\omega_s^2}{\omega_m^2}\right), \tag{8}$$

where ω_s in (7) and (8) is given by (5) for a cylindrical RF trap.

Numerical simulations [16] are in good agreement with these results. Furthermore, it is worthwhile to note that this model applies in every experimental case described by Cutler et al. [17, 18] when the charge density distribution is Gaussian. The physical parameters that have to be determined experimentally are the total number of ions N and the secular frequency $\omega_m/2\pi$.

In this paper N is determined by the method of image currents [19] and $\omega_m/2\pi$ is measured directly in the first-order Doppler spectrum of the hyperfine transition. The precision obtained on the second-order Doppler shift by this method is also discussed.

1. Experimental Set-up and Results

1.1. First-Order Doppler Spectrum of the Microwave Hyperfine Transition of the Fundamental Level $^2S_{1/2}$ of ^{199}Hg Stored Ions in an RF Cylindrical Trap

The experimental set up has been described elsewhere [14, 20]. The radius of the cylindrical trap is $r_0=19$ mm and its half height $z_0=r_0/\sqrt{2}=13.4$ mm. It is kept in a vacuum system whose base pressure is $7\cdot10^{-10}$ Torr and increases up to $8\cdot10^{-9}$ Torr when neutral mercury is introduced in the system by a variable leak.

Good vacuum conditions are necessary in order to enhance storage lifetimes by decreasing radiofrequency heating effects due to collisions of stored ions with neutral mercury. Storage times of about 4 s are achieved without any buffer gas in the trap. The mean storage lifetime is easily measured by observing the variation of the fluorescence at 194.2 nm between the $^2P_{1/2}$ and the $^2S_{1/2}$ states of $^{199}Hg^+$ stored ions illuminated by an $^{199}Hg^+$ lamp when the V_{DC} trapping voltage is modulated. During the first half period of 5 s V_{DC} equals 12 V while it becomes -27 V during the next half period. Meanwhile V_{AC} and Ω are kept constant with the following values:

$$V_{AC}=300\text{ V} \quad \text{and} \quad \Omega/2\pi\sim 260\text{ kHz}.$$

According to the stability diagram [6], ion storage is only possible in the first half period. The slope of the increase of the fluorescence signal observed in this way (Fig. 1) gives the mean storage lifetime, which, under these conditions, is 4 s.

In order to observe the hyperfine resonance at 40.5 GHz, we use the classical scheme of optical and

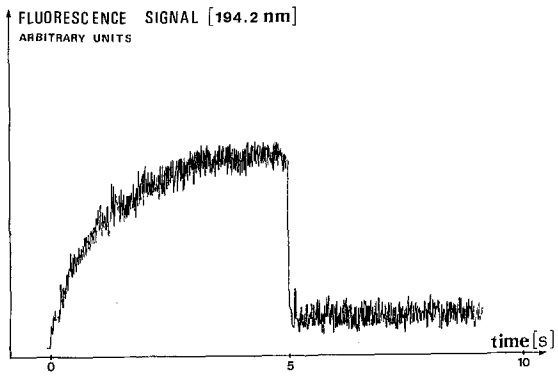

Fig. 1. Variation of the stored ions fluorescence signal at 194.2 nm when the constant trapping voltage V_{DC} is modulated

microwave double resonance. A $^{202}Hg^+$ lamp produces the optical pumping of 194.2 nm, while the microwave signal is generated by frequency multiplication and synthesis from a 5 MHz quartz oscillator.

At sufficiently low microwave power we obtain high resolution resonances (Fig. 2) whose quality factor is

$$Q = \nu/\delta\nu = 5.4 \cdot 10^9 .$$

The signal intensity is about 10% of the background.

At maximum microwave power ($\sim \frac{1}{2}$ mW) the broadening of the central line is about 340 Hz while first-order Doppler sidebands now become well observable under these conditions the saturation factor of the central line is 650.

We have studied the second-order Doppler shift of the hyperfine resonance in two different experimental situations with spherical pseudopotential wells.

i) The RF drive is of 340 V at $\Omega/2\pi \simeq 260$ kHz and $V_{DC} = 31$ V. The resulting single ion secular frequency according to (5) is $\omega_s/2\pi = 50$ kHz and the pseudopotential depth (Fig. 3) is $D_0 \simeq 6$ eV. Note that for the values of $z > 11$ mm the ions are ejected towards the trap electrodes by the trapping potential itself. The pseudopotential is spherically symmetric within a sphere of radius 6 mm from the central space of the trap.

The first-order Doppler spectrum observed is depicted in Fig. 4.

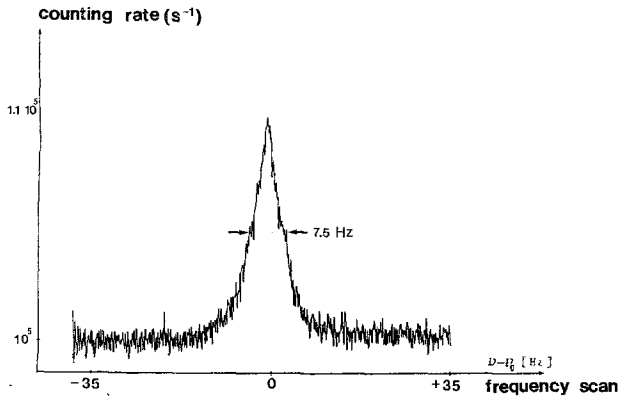

Fig. 2. Hyperfine resonance of the fundamental level $^2S_{1/2}$ at 40.507348 GHz of stored $^{199}Hg^+$ ions in an RF cylindrical trap

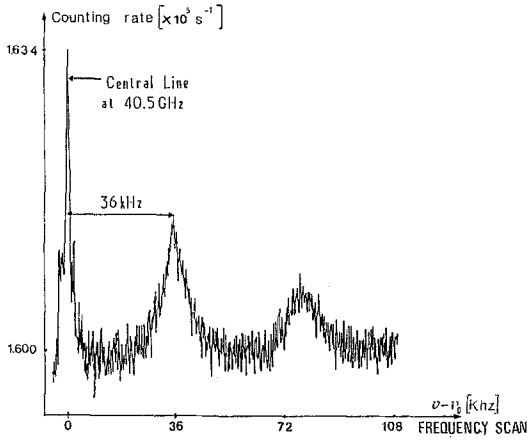

Fig. 4. Microwave hyperfine spectrum of the fundamental level $^2S_{1/2}$ of $^{199}Hg^+$ at 40.507348 GHz modulated at the ion secular frequency shifted by space charge effects: $\omega_m/2\pi = 36$ kHz. The effective potential is at 50 kHz

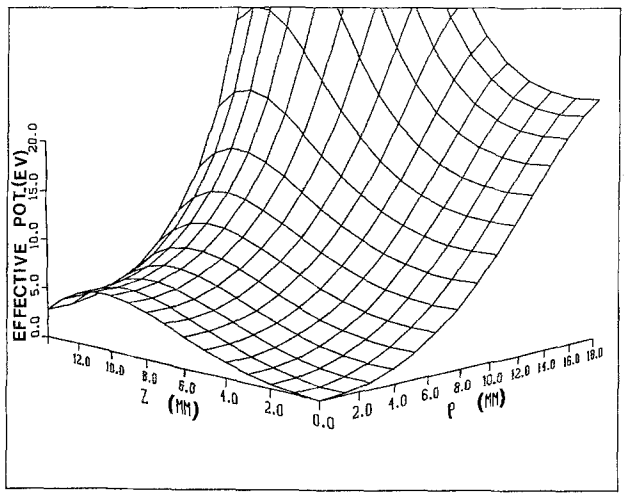

Fig. 3. Effective potential of an RF cylindrical trap with the following trapping parameters: $V_{DC} = 31$ V; $V_{AC} = 340$ V; $\Omega/2\pi = 260$ kHz. The depth of the pseudopotential is: $D_0 = 6$ eV. The single ion theoretical secular frequency in the central space of the trap where the potential is spherically symmetrical is: $\omega_s/2\pi = 50$ kHz

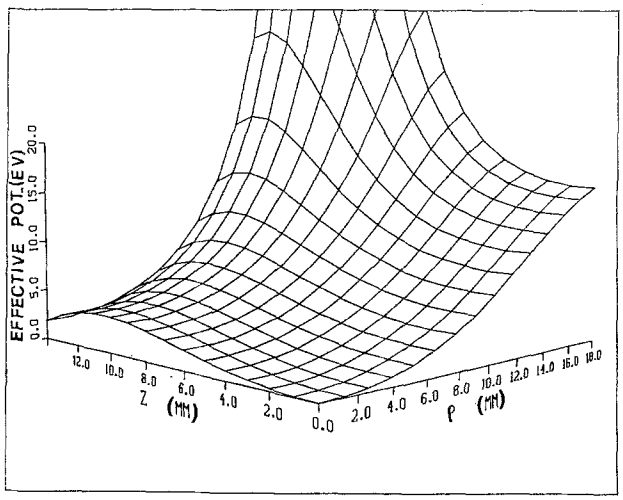

Fig. 5. Effective potential of an RF cylindrical trap with the following trapping components: $V_{DC} = 20$ V; $V_{AC} = 276$ V; $\Omega/2\pi = 260$ kHz. The pseudopotential well depth is: $D_0 = 4.5$ eV. The single ion theoretical secular frequency in the central volume of the trap where the potential is spherically symmetrical is: $\omega_s/2\pi = 40$ kHz

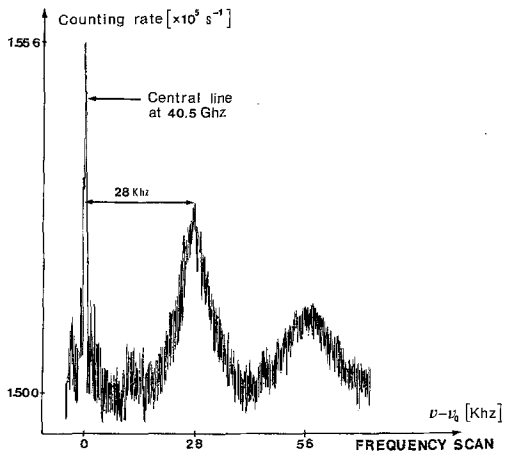

Fig. 6. Microwave hyperfine spectrum of the fundamental level $^2S_{1/2}$ of $^{199}Hg^+$ at 40.507348 GHz in a spherical effective potential of $\omega_s/2\pi = 40$ kHz, modulated at the ion secular frequency reduced by space charge effects: $\omega_m/2\pi = 28$ kHz

The measured secular frequency determined by the lateral lines is $\omega_m/2\pi = 36\,\text{kHz} > \frac{1}{2}(\omega_s/2\pi)$ from which we deduce that the central density of the so-formed ion cloud is [8]:

$$n(0) = m\varepsilon_0(\omega_s^2 - \omega_m^2)/|\mu| q^2 \sim 2.3 \cdot 10^{13}\,\text{m}^{-3}. \quad (9)$$

ii) The RF drive is $V_{AC} = 276$ V at $\Omega/2\pi \sim 260$ kHz and $V_{DC} = 20$ V. Thus $\omega_s/2\pi = 40$ kHz and $D_0 \simeq 4$ eV (Fig. 5). As previously the sphericity of this potential occurs within a sphere of radius 6 mm. The hyperfine spectrum observed is given in Fig. 6.

The measured secular frequency is $\omega_m/2\pi = 28\,\text{kHz} > \frac{1}{2}\left(\frac{\omega_s}{2\pi}\right)$. The central density of the ion cloud is about $1.6 \cdot 10^{+13}\,\text{m}^{-3}$.

1.2. Experimental Determination of the Total Number of Ions; Temperature and Second-Order Doppler Shift Estimation

The total number of ions is measured by applying a modulated signal near ω_m between the two endcaps of the trap and observing image currents induced in the trap electrodes by the ion cloud motion. When the sweep rate is lower than $\sim 100\,\text{rad} \cdot \text{s}^{-2}$ the surface of the detected signal is directly proportional to the total number of ions N according to the relation [19]:

$$N = \left(\frac{Y_{max} \Delta\omega}{b}\right)\left(\frac{4mz_0^2}{q^2 \Gamma^2}\right)\left(\frac{1 + R_f G_0}{R_f}\right), \quad (10)$$

with

$$b = (2 - \tfrac{3}{2} Y_{max})^{1/2}/(2 - \tfrac{1}{2} Y_{max})^{1/2},$$

where Y_{max} and $\Delta\omega$ characterize respectively the signal amplitude and width while m and q are the ion mass and charge. G_0 is the admittance of the resonant circuit and Γ a factor to account for the fact that the mean field is not simply $v/2z_0$ where v is the probing voltage on the endcaps electrodes [21].

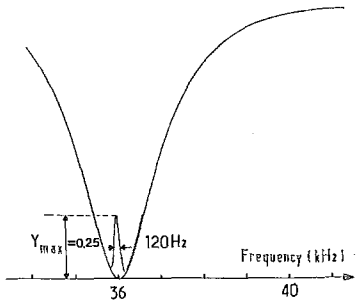

Fig. 7. Ion number signal at 36 kHz in the case of a 50 kHz spherical effective potential

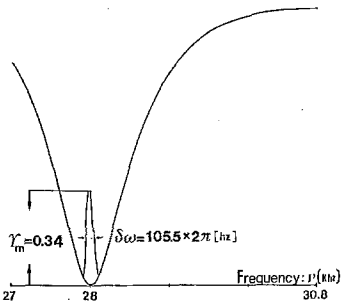

Fig. 8. Ion number signal at 28 kHz in the case of a 40 kHz spherical effective potential

Complete calculation of Γ for different values of the ratio of the potential well depth to the thermal kinetic energy of the ions is given in [19]. For our experimental conditions $D_0/(\frac{3}{2}K_B T) \sim 10$ so that we can consider that $\Gamma \simeq 1$. The uncertainty in the measurement of N comes essentially from ΔY_{max} and $\Delta\omega$ and is about 6%.

In the case of a 50 kHz pseudopential well $Y_{max} = 0.25 \pm 0.01$ and $\Delta\omega/2\pi = (120 \pm 2)$ Hz (Fig. 7) with $b = 0.93$, $R_f = 2M\Omega$ and $G_0 = 4.9 \cdot 10^{-7}\,\Omega^{-1}$ we obtain $N = (1.9 \pm 0.1) \cdot 10^6$ ions.

Using (4) and (5) one obtains the ion cloud temperature

$$T = 3580 \pm 120\,\text{K}$$

and the second-order Doppler shift

$$\frac{\Delta f}{f} = -(5.70 \pm 0.18) \cdot 10^{-12}.$$

The contribution of the second-order Doppler effect to the total error is less than $2 \cdot 10^{-13}$. The radius of the ion cloud as defined in (6) is, under these conditions, $R = 2.4$ mm.

For the 40 kHz pseudopotential well the observed signal of the ion number is presented in Fig. 8, where

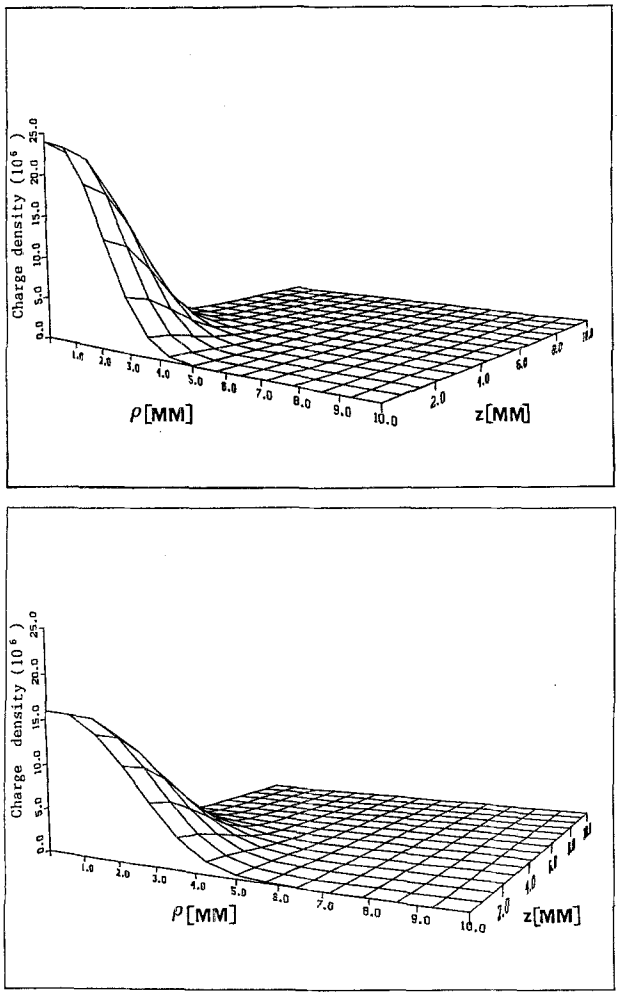

Fig. 9a, b. Comparison of the charge density distribution of the ion cloud in the 50 kHz effective potential **a** and the 40 kHz effective potential **b** deduced from computation of (11) and (12) with the values of $n(0)$ and T determined by the previous semi-empirical method

$Y_{max}=0.34\pm0.01$ and $\Delta\omega/2\pi=(105.5\pm2)$ Hz we obtain $N=(2.3\pm0.1)\cdot10^6$ ions.

We then have according to (4) and (5):

$$T=3315\pm90\,\mathrm{K} \quad \text{and} \quad \frac{\Delta f}{f}=-(5.44\pm0.16)\,10^{-12}.$$

The ion cloud radius is $R=3$ mm.

Note that in this case we have a larger ion number at almost the same temperature but with a lower value of central density. This is due to the fact that the secular frequency of the effective potential is lower, thus permitting the ions to oscillate at bigger amplitudes, consequently giving a bigger ion cloud radius (Fig. 9).

The secular frequency $\omega_{m\varrho}/2\pi$ measured in the first-order Doppler spectrum corresponds to the ion oscillation along $\varrho=(x^2+y^2)^{1/2}$ direction while that detected by image currents $\omega_{mz}/2\pi$ corresponds to the oscillation along z axis of the trap.

It becomes evident that a combination of these two experimental methods can give information about the influence of trap asymmetry on the sphericity of the ion cloud. In our case the trap asymmetry comes essentially from the holes on the cylindrical electrode for the optical pumping and the microwave excitation. In the previous examples a slight difference, less than 2%, has been observed between $\omega_{m\varrho}$ and ω_{mz}, showing that the effect of trap asymmetry is small. This can be explained in the case of a cylindrical RF trap by the high values of the effective potential along ϱ axis which partially compensates the irregularities due to the holes.

2. Comparison with Numerical Computation

The rigorous equation describing the thermal equilibrium of N ions in a spherical pseudopotential at temperature T taking into account space charge effects is:

$$N=2\pi n(0)\int_{-\infty}^{+\infty}\int_{0}^{+\infty}\varrho\exp\{-[V_{eff}(\varrho,z)+q\Phi_{sc}(\varrho,z)-q\Phi_{sc}(0,0)]/k_BT\}\,d\varrho dz \tag{11}$$

where the charge density distribution is assumed Maxwellian and $V_{eff}(\varrho,z)$ is given by (3) with $\{V_{DC}, V_{AC}, \Omega\}$ satisfying (4). $\Phi_{SC}(\varrho,z)$ is the space charge potential satisfying Poisson's equation in cylindrical coordinates:

$$\frac{1}{\varrho}\frac{\partial}{\partial\varrho}\left(\varrho\frac{\partial\Phi_{sc}(\varrho,z)}{\partial\varrho}\right)+\frac{\partial^2\Phi_{sc}(\varrho,z)}{\partial z^2}=-\frac{qn(0)}{\varepsilon_0}\exp\left\{-\frac{V_{eff}(\varrho,z)+q(\Phi_{sc}(\varrho,z)-\Phi_{sc}(0,0)}{K_BT}\right\}, \tag{12}$$

where conventionally we have taken $V_{eff}(0,0)\equiv0$ and $\Phi_{sc}(r_0,z_0)\equiv0$.

A method to test the previous results is to insert the determined values of $n(0)$ and T in (12) and (11), compute the system of equations and compare the resulting theoretical value of N to that measured experimentally.

– In case i) we obtain $N=1.84\cdot10^6$ ions which is very close to the experimentally determined value $N=(1.9\pm0.1)\,10^6$,

– In case ii), we find $N=2.33\cdot10^6$ ions which is equally close to the experimental value $(2.3\pm0.1)\,10^6$.

This demonstrates that the approximate analytical expressions [8] combined with experimentally measured parameters describe remarkably well the energy properties of a thermalized ion cloud.

3. Conclusion

We have shown that we can estimate the second-order Doppler shift in stored ions hyperfine microwave spectroscopy by applying a new semi-empirical method using an analytical model with experimentally measured physical parameters. The obtained precision is of the same order as previous [16, 18] numerical simulation methods. The practical aspect of this method is quite evident and can be applied in all kinds of experimental situations with spherical effective potential in an RF trap.

References

1. W. Paul, O. Osberghaus, E. Fischer: Forschungsber. Wirtch. Verkehrsministeriums. Nordrhein-Westfalen, No. 45 (1958)
2. H.G. Dehmelt: *Advances in atomic and molecular physics*, Vol. 3 (Academic, New York 1967) p. 53
3. H. Lagadec, C. Meis, M. Jardino: Int. J. Mass Spectr. Ion Processes (April 1988) (accepted)
4. R.F. Bonner, J.E. Fulford, R.E. March, G.F. Hamilton: Int. J. Mass Spectr. Ion Processes **24**, 255 (1977)
5. A. Angot: Compléments de Mathématique (Masson, 1972) 6ème éd. Sect. 77
6. M.N. Benilan, C. Audoin: Int. J. Mass Spectr. Ion Processes **11**, 421–432 (1973)
7. A. Gaponov, M.A. Miller: JETP October 15 (1957)
8. C. Meis, M. Desaintfuscien, M. Jardino: Appl. Phys. B **45**, 59–64 (1988)
9. F. Vedel, J. André, M. Vedel: J. de Phys. **42**, 1611 (1981)
10. R.H. Dicke: Phys. Rev. **89**, 472 (1953)
11. H.A. Schuessler, E.N. Fortson, H.H.G. Dehmelt: Phys. Rev. **187**, 5 (1969)
12. F.G. Major, G. Werth: Phys. Rev. Lett. **23**, 1155 (1973)
13. D.J. Wineland: Proc. 11th Annual P.T.T.I. Appl. of Planning Meeting (1979), NASA, Conf. Publ. 2129, p. 81
14. M. Jardino, M. Desaintfuscien, R. Barillet, J. Viennet, P. Petit, C. Audoin: Appl. Phys. **24**, 107 (1981)
15. L.S. Cutler, R.P. Gilford, M.D. McGuire: Proc. 37th Annual Symposium on Frequency control, p. 32 (1983)
16. M. Jardino, M. Desaintfuscien, F. Plumelle, J.L. Duchêne: Proc. 38th Annual Symposium on frequency control (1984). IEEE Press 84 CH 2062-8, p. 431
17. L.S. Cutler, R.P. Giffard, M.D. McGuire: Appl. Phys. B **36**, 137–142 (1985)
18. L.S. Cutler, R.P. Giffard, M.D. McGuire, C.A. Flory: Appl. Phys. B **39**, 251–259 (1986)
19. M.N. Gaboriaud, M. Desaintfuscien, F.G. Major: Int. J. Mass Spectr. Ion Processes **41**, 109–123 (1981)
20. C. Meis, M. Jardino, M. Desaintfuscien: 2nd European Frequency and Time Forum, Neuchâtel, March 1988
21. D.J. Wineland, H.G. Dehmelt: J. Appl. Phys. **46**, 919 (1975)